Dora M. Berman,[1,2] R. Damaris Molano,[1] Carmen Fotino,[1] Ulisse Ulissi,[1] Jennifer Gimeno,[1] Armando J. Mendez,[1,3] Norman M. Kenyon,[1,2] Norma S. Kenyon,[1,2,4,5] David M. Andrews,[6] Camillo Ricordi,[1,2,3,4,5] and Antonello Pileggi[1,2,4,5]

Bioengineering the Endocrine Pancreas: Intraomental Islet Transplantation Within a Biologic Resorbable Scaffold

Diabetes 2016;65:1350–1361 | DOI: 10.2337/db15-1525

Transplantation of pancreatic islets is a therapeutic option to preserve or restore β-cell function. Our study was aimed at developing a clinically applicable protocol for extrahepatic transplantation of pancreatic islets. The potency of islets implanted onto the omentum, using an in situ–generated adherent, resorbable plasma-thrombin biologic scaffold, was evaluated in diabetic rat and nonhuman primate (NHP) models. Intraomental islet engraftment in the biologic scaffold was confirmed by achievement of improved metabolic function and preservation of islet cytoarchitecture, with reconstitution of rich intrainsular vascular networks in both species. Long-term nonfasting normoglycemia and adequate glucose clearance (tolerance tests) were achieved in both intrahepatic and intraomental sites in rats. Intraomental graft recipients displayed lower levels of serum biomarkers of islet distress (e.g., acute serum insulin) and inflammation (e.g., leptin and α2-macroglobulin). Importantly, low-purity (30:70% endocrine:exocrine) syngeneic rat islet preparations displayed function equivalent to that of pure (>95% endocrine) preparations after intraomental biologic scaffold implantation. Moreover, the biologic scaffold sustained allogeneic islet engraftment in immunosuppressed recipients. Collectively, our feasibility/efficacy data, along with the simplicity of the procedure and the safety of the biologic scaffold components, represented sufficient preclinical testing to proceed to a pilot phase I/II clinical trial.

Intrahepatic islet transplantation has been the gold standard for clinical islet transplantation trials aimed at treating patients with type 1 diabetes (T1D) and hypoglycemia unawareness or with surgically induced diabetes (pancreatectomy) (1). It has resulted in normalization of hemoglobin A_{1c}, improved glycemic control, and elimination of severe hypoglycemic events, even in the absence of insulin independence (2). Progressive graft dysfunction has been observed in clinical trials years after intrahepatic islet transplantation, often requiring reintroduction of exogenous insulin. Long-term intrahepatic islet dysfunction has been also observed in preclinical models (3). Activation of an immediate blood-mediated inflammatory reaction (IBMIR) and hypoxia in the transplant microenvironment after intrahepatic islet embolization contributes to functional impairment and the loss of a significant portion of the transplanted islets (4–7). Furthermore, the hepatic first pass of orally administered drugs exposes intrahepatic islets to higher concentrations of diabetogenic immunosuppressive agents. Other potential challenging factors in this setting include accumulation of peri-insular fat (microsteatosis) in the liver parenchyma (8–13). Moreover, chronic exposure of intrahepatic islets to endotoxins and other proinflammatory agents absorbed through the gastrointestinal tract, in addition to the IBMIR, may trigger adaptive immune responses that are known to be associated with a higher

[1]Cell Transplant Center, Diabetes Research Institute, University of Miami, Miami, FL
[2]The DeWitt Daughtry Family Department of Surgery, University of Miami, Miami, FL
[3]Department of Medicine, University of Miami, Miami, FL
[4]Department of Microbiology and Immunology, University of Miami, Miami, FL
[5]Department of Biomedical Engineering, University of Miami, Miami, FL
[6]Department of Pathology, University of Miami, Miami, FL

Corresponding author: Dora M. Berman, dberman2@med.miami.edu; Camillo Ricordi, ricordi@miami.edu; or Antonello Pileggi, antonello.pileggi@nih.gov.

Received 4 November 2015 and accepted 17 February 2016.

Clinical trial reg. no. NCT02213003, clinicaltrials.gov.

A.P. is currently affiliated with the Center for Scientific Review, National Institutes of Health, Bethesda, MD.

D.M.B., R.D.M., C.R., and A.P. equally contributed.

incidence of acute and chronic rejection episodes, as well as possibly facilitate recurrence of autoimmunity in transplanted subjects with T1D (2).

The final objective of developing an extrahepatic site for islet transplantation is not only the ability to provide physiologic portal drainage of endocrine pancreas secretions but also the possibility of engineering the transplant microenvironment for the development of successful biologic replacement strategies that could avoid the need for chronic recipient immunosuppression (14,15). Ideal characteristics of such a site include sufficient space to accommodate relatively large tissue volumes (e.g., low-purity or encapsulated insulin-producing cell products), allow for minimally invasive transplant procedures, and enable noninvasive longitudinal monitoring and access for graft biopsy and/or retrieval, as well as physiologic venous drainage through the portal system (14,15). An additional advantage is the reportedly immunomodulatory effect of antigens delivered though the portal venous system (portal tolerance) that was associated with lower rejection rates in pancreas transplants with portal versus systemically drained organs (16).

The omentum is easy to mobilize and adequately large to accommodate islet grafts (300–1,500 cm^2 surface area in humans) (17,18). It is composed of two mesothelial sheets containing rich capillary networks draining into the portal venous system (19–21). Furthermore, intraomental islet implantation was shown to improve metabolic control in diabetic animal models (22,23).

We engineered a biologic scaffold by using plasma and recombinant human thrombin (rhT), a serine protease (factor IIa in the coagulation cascade) that catalyzes the conversion of plasma fibrinogen into fibrin that polymerizes forming a clot. The intraomental site was tested by implanting islets, embedded in situ into the resorbable biologic scaffold, on the omentum of diabetic rat and nonhuman primate (NHP) models with streptozotocin-induced diabetes. Our data support the feasibility of the approach that is currently in phase I/II clinical trials.

RESEARCH DESIGN AND METHODS

Animals

Studies involving animal subjects were performed under protocols approved and monitored by the University of Miami (UM) Institutional Animal Care and Use Committee. Animals were housed at the Division of Veterinary Resources. Lewis (MHC, rat haplotype: $RT1^l$) and Wistar Furth (WF) ($RT1^u$) rats (http://www.harlan.com) were used as islet donors (>250 g males) and Lewis rats as recipients (170–200 g females). For selected experiments, rats with an indwelling jugular vein catheter (JVC) were purchased. Rodents were housed in microisolated cages with free access to autoclaved water and food. Both donor and recipient cynomolgus monkeys (7.92 and 3.58 years old, respectively) were obtained from the Mannheimer Foundation (Homestead, FL) and were specific pathogen free. Pair-housed monkeys were supplied with water ad libitum and fed twice daily (24). UM holds Animal Welfare Assurance A-3224-01, effective 12 April 2002, with the Office of Laboratory Animal Welfare, National Institutes of Health, and is accredited by the Association for Assessment and Accreditation of Laboratory Animal Care.

Diabetes Induction and Metabolic Monitoring

Diabetes was induced by administration of streptozotocin at 60 mg/kg i.p. in rats (2 injections 2–3 days apart; Sigma-Aldrich) (25) and 100 mg/kg i.v. in NHP (Tevapharm.com) (7,22).

Rodents with nonfasting glycemic values ≥300 mg/dL on whole blood samples obtained from tail pricking (OneTouch Ultra glucometers [http://www.lifescan.com]) were used as recipients. Graft function was defined as nonfasting glycemia <200 mg/dL. At selected time points after transplantation, a glucose tolerance test was performed in rodents to evaluate graft potency (25). After overnight fasting, an oral (oral glucose tolerance test [OGTT]; 2.5 g/kg) or intravenous (intravenous glucose tolerance test [IVGTT]; 0.5 g/kg) glucose bolus was administered, and glycemic values were monitored with portable glucometers. The area under the curve (AUC) of glucose was calculated as previously described (26). In the case of allogeneic islet transplants, return to nonfasting hyperglycemic state was considered a sign of graft rejection.

In NHP, diabetes was defined as fasting C-peptide levels <0.2 ng/mL and a negative response (stimulated C-peptide <0.3 ng/mL) to a glucagon challenge performed 4 weeks after streptozotocin treatment (7,22). Heel-stick glycemic values were monitored two to three times daily (OneTouch Ultra). Subcutaneous insulin (Humulin R [https://www.lilly.com] or Humulin R plus Lantus [http://www.sanofi.us]) was administered based on an individualized sliding scale as needed, aiming for fasting blood glucose (FBG) and postprandial plasma blood glucose (PBG) levels of 150–250 mg/dL poststreptozotocin and prior to transplantation. Plasma C-peptide levels were assessed by electrochemiluminescence immunoassay using a Cobas analyzer (https://usdiagnostics.roche.com).

Plasma Collection

Blood obtained from venipuncture was collected into microcentrifuge tubes containing 3.2% sodium citrate. Plasma was obtained after centrifugation at 1,455*g* for 10 min at room temperature, and aliquots were stored at −80°C and thawed before use.

Islet Isolation and Graft Preparation

Islets were obtained by enzymatic digestion, followed by purification on density gradients using protocols standardized at the Diabetes Research Institute (DRI) for rats (DRI Translational Core) (27), NHP (22), and humans (DRI cGMP Human Cell Processing Facility) (1,28–30).

For evaluation of the effect of the degree of islet preparation purity on intraomental engraftment and function, Lewis rat islets were isolated and purified using a standard technique (27), yielding >95% purity (pure

fraction) as assessed by dithizone staining (Sigma-Aldrich) (1,2). The pancreatic slurry containing exocrine tissue clusters (lowest purity fraction) after islet purification was maintained in culture and counted with the algorithm used to determine islet equivalents (IEQ) (2). Before transplantation, an aliquot of the final pure islet product was mixed with the exocrine pancreatic tissue to obtain a 30% pure islet cell product (3:7 v/v, islet vs. exocrine tissue).

Islet Transplantation

Under general anesthesia, a substernal midline minilaparotomy allowed exteriorizing the omentum that was spread flat over a sterile field (Fig. 1). We previously reported a similar intraomental flap transplant procedure in NHP (22).

The rhT (Recothrom, National Drug Code no. 28400 [http://www.zymogenetics.com]) was reconstituted with the 0.9% NaCl included in the kit for rodents or with Dulbecco PBS with Ca^{2+}/Mg^{2+} (GIBCO [http://www.thermofisher.com]) in the NHP experiment. Final aliquots of rhT (1,000 IU/mL) were stored at −20°C.

The transplantation procedure with the in situ generation of the islet-containing biologic scaffold is summarized in Fig. 1. For rodent experiments, islet aliquots were centrifuged (1 min, 200*g*), supernatant was discarded, and islets were resuspended in syngeneic (autologous) plasma. After another centrifugation, most of the excess plasma was removed and the slurry of islets/plasma collected with a precision syringe (hamiltoncompany.com). Similarly, in the case of the NHP, islets were collected into a microcentrifuge tube, quick spun and washed twice in donor plasma (obtained on day −1, stored at 4°C), and transported to the operating room. Plasma excess was removed before collection of islets/plasma with use of a micropipette (P1000). In both species, the islets/plasma slurry was gently distributed onto the surface of the omentum (Fig. 1*A*, *b2*, and *c3*) and then rhT gently dripped onto the graft (Fig. 1*A*, *c4*), resulting in immediate gelling and adherence of the islets to the omental surface. The omentum was gently folded on itself to increase contact with and containment of the graft (Fig. 1*A*, *b3*, *b4*, and *c5*). In the NHP, nonresorbable sutures were placed on the omentum outside the graft area as reference for the time of retrieval (Fig. 1, *c5*). In rodent experiments, nothing, sutures, or a plasma: rhT mix (10:1 v/v) was used on the folded omentum. After repositioning the omentum into the peritoneal cavity, abdominal wall muscle and skin were sutured.

To avoid the potential confounding effect of variability in islet preparations (31), for rat experiments aimed at comparison of transplant sites or purity, equal numbers of syngeneic islets, from large batch isolations, were implanted in parallel into diabetic recipients in a biologic scaffold or into the liver (25). In selected rats, survival surgery to remove graft-bearing omentum after long-term follow-up was performed to confirm prompt return to hyperglycemia, thereby ruling out residual function of native endocrine pancreas.

Immunosuppression

Clinically relevant immunosuppressive agents were used in both rat and NHP allogeneic transplant models (32–35). Rats received induction treatment with antilymphocyte serum (0.5 mL i.p. on day −3 [http://www.accurate

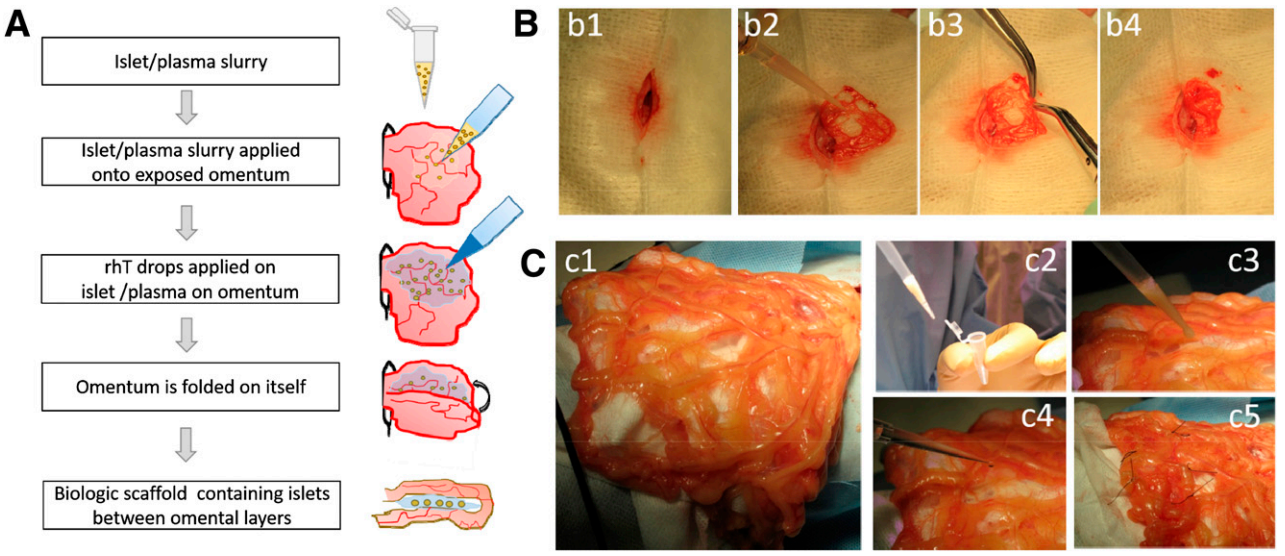

Figure 1—Intraomental islet implantation within a biologic scaffold. *A*: Schematic diagram of the transplant procedure. *B*: Procedure in rat. *C*: Procedure in NHP. After midline laparotomy (*b1*), the omentum is gently exteriorized and opened (*b2* and *c1*). The islet graft, resuspended in autologous plasma (*c2*), is gently distributed onto the omentum (*b3* and *c3*). Recombinant human thrombin is added onto the islets on the omental surface to induce gel formation (*c4*), and then the omentum is folded to increase the contact of the graft to the vascularized omentum (*b4* and *c5*). Nonresorbable stitches were placed on the far outer margins of the graft in the NHP (*c5*) for easier identification of the graft area at the time of graft removal.

.com.gr]) and mycophenolic acid (20 mg/kg/day starting on the day of transplant for 2 weeks then tapered by one-quarter of the dose every 2 days until day 20; Myfortic [https://www.novartis.com]) (36) combined with cytotoxic T-lymphocyte–associated protein-4 (CD152)–immunoglobulin fusion protein (CTLA4Ig) (10 mg/kg i.p. on days 0, 2, 4, 6, 8, and 10 and weekly thereafter; abatacept [Orencia] [http://www.bms.com]), adapted from Safley et al. (35). The NHP received anti-thymocyte (rabbit) globulin (10 mg/kg i.v. on days −1, 0, 2, and 4 from transplant; thymoglobulin; Sanofi), CTLA4Ig (20 mg/kg i.v. on days 0, 4, 14, 28, 56, and 75 and monthly thereafter at 10 mg/kg; belatacept [Nulojix] [http://www.bms.com]), and sirolimus (daily from day 2, aiming at trough levels of 8–12 ng/mL; rapamycin [http://www.lclabs.com]).

Biomarkers

Blood samples were collected from indwelling JVC at baseline and after selected time points posttransplant. Insulin, C-peptide, leptin, interleukin (IL)-6, and chemokine (C-C motif) ligand 2 (CCL2) (formerly MCP-1) were measured using commercial multiplex kits (http://www.emdmillipore.com) and analyzed on a Luminex system. Levels of the rat acute-phase proteins α2-macroglobulin and haptoglobin were measured using specific ELISA kits (http://www.lifediagnostics.com) on a kinetic microplate reader (SoftMaxPro version 5; https://www.moleculardevices.com).

Histopathology

Tissue sections (4 μm thick) were stained with hematoxylin-eosin for morphologic assessment of the grafts. Masson trichrome staining (Chromaview, Richard-Allan Scientific [https://vwr.com]) was performed on selected grafts to reveal collagen (blue stain) or muscle fibers and cytoplasm (red stain) (25). Immunofluorescence was performed using specific antibodies to detect insulin (1:100; guinea pig anti-insulin [http://www.dako.com]), glucagon (GCG) (1:100; rabbit anti-glucagon [http://www.biogenex.com]), endothelium (1:20; rabbit anti-CD31 [http://www.abcam.com] or 1:50; von Willebrand factor [vWF], rabbit anti-vWf [http://www.emdmillipore.com]), smooth muscle actin (SMA) (1:50; rabbit anti-SMA [http://www.abcam.com]), and T cells (1:100; CD3, rabbit polyclonal anti-human [http://www.cellmarque.com]). Secondary antibodies used were goat anti–guinea pig Alexa Fluor 568 (1:200) and goat anti-rabbit Alexa Fluor 488 (1:200; Invitrogen [http://www.thermofisher.com]). Digital images were acquired using an SP5 inverted confocal microscope (http://www.leica.com) at the DRI Imaging Core Facility.

Scanning Electron Microscopy

Human plasma was obtained from volunteers who gave consent (IRB20091138). Human islets and plasma/thrombin clots with or without human islets were fixed in 2% glutaraldehyde in PBS (0.137 mol/L NaCl, 0.01 mol/L Na_2HPO_4, and 0.0027 mol/L KCl, pH 7.4) for ≥3 h and stored in fixative at 4°C. After three washes, samples were postfixed with 1% osmium tetroxide in PBS, dehydrated in ethanol, dried with hexamethyldisilazane, dispersed in plastic weigh boats, and outgassed overnight. Preparations were adhered by gentle tapping with an aluminum stub, covered with a carbon adhesive tab, and then coated with a 20-nm-thick layer of palladium in a plasma sputter coater and imaged at the UM Center for Advanced Microscopy using a field emission scanning electron microscope (FEI XL-30).

Statistical Analysis

Data were analyzed using Excel (https://www.microsoft.com), SigmaPlot (http://www.sigmaplot.com), and Prism6 (http://www.graphpad.com). Shapiro-Wilk test was used to assess parametric data distribution. An unpaired *t* test was performed to compare experimental groups. Values shown are mean ± SEM, except where indicated. *P* values <0.05 were considered statistically significant.

RESULTS

Ultramicroscopic Structure of the Biologic Scaffold

Scanning electron microscopy revealed the intricate net of fibrin fibers obtained through the reaction triggered by rhT in human plasma (Fig. 2*A*). Human islet cell surface appeared smooth by ultramicroscopy (Fig. 2*B*). The clot induced by combining human plasma with rhT and human islets in vitro resulted in the development of an orthomorphic three-dimensional fibrin matrix trapping islet structures within the newly formed biologic scaffold (Fig. 2*C*). We reasoned that the induction of the plasma/thrombin reaction to create a microscopic, adherent fibrin scaffold around the implanted islets would be useful to promote islet graft adhesion on the surface of the omentum, preventing islet pelleting, and therefore aiding engraftment, neovascularization, and islet survival.

Intraomental Islets Transplanted Into Biologic Scaffolds Restore Normoglycemia in Diabetic Rats

We used a syngeneic rat islet transplant model. We previously demonstrated that streptozotocin diabetic recipients of 3,000 IEQ experienced reversal of diabetes after either intra- or extrahepatic transplantation (25). After intraomental transplantation of 17,338 ± 881 IEQ/kg, all animals (n = 7; 173.4 ± 91 g body wt) achieved normoglycemia within 2 days and maintained euglycemia during the follow-up period (Fig. 3*A*), even >200 days. Two animals underwent removal of the graft-bearing omentum on day 76 posttransplantation: one died after surgery and the other promptly become hyperglycemic (Fig. 3*A*). The rest of the recipients was followed for >200 days posttransplantation. IVGTT performed in selected animals 2 months after islet transplantation showed that transplanted islets cleared glucose within 75 min after receiving a glucose bolus in a fashion comparable with that of naïve animals (n = 3/group; AUC 17,851 ± 810 mg × min × dL^{-1} in naïve rats vs. 16,276 ± 857 mg × min × dL^{-1} in intraomental islet biologic scaffold recipients) (Fig. 3*B*). Furthermore, OGTT performed on transplanted animals at 11 and 26 weeks postimplantation confirmed

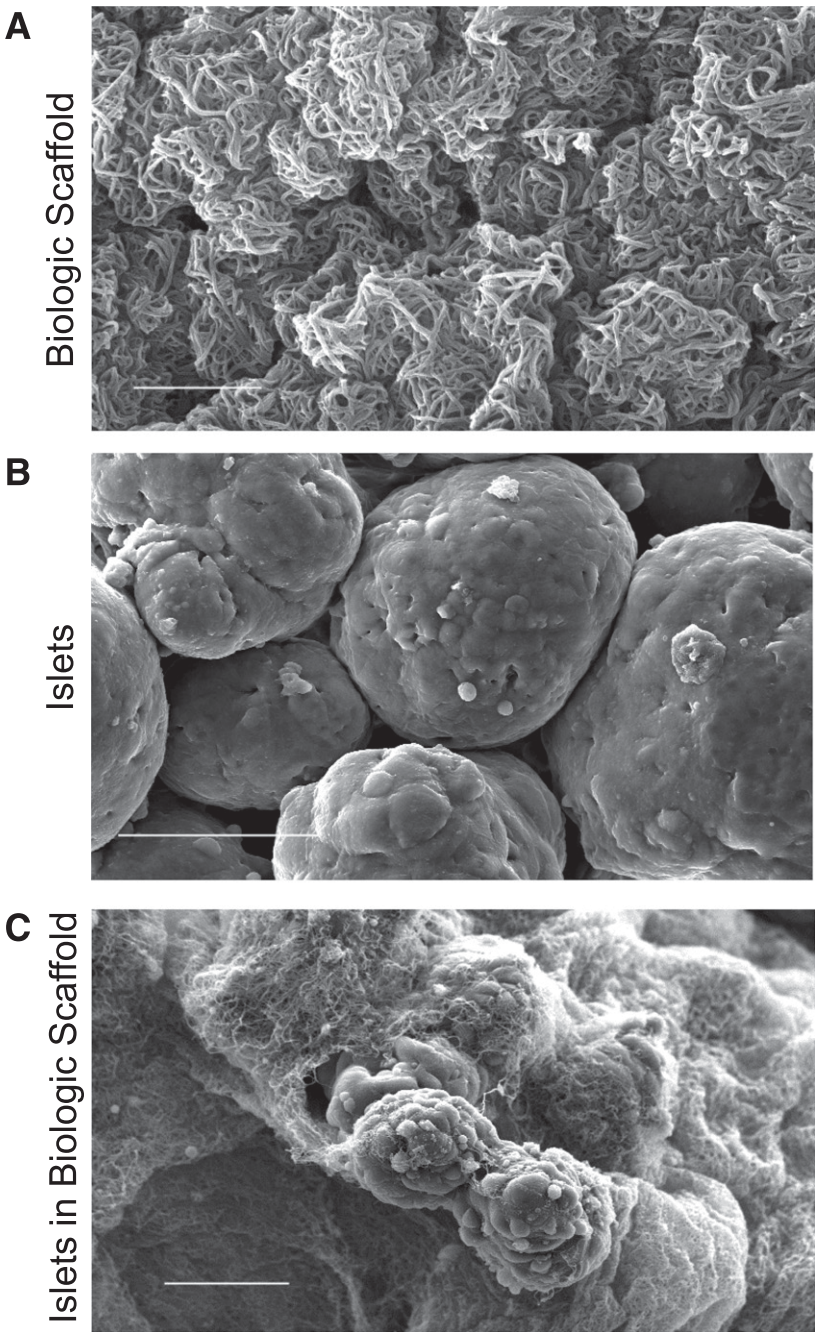

Figure 2—Scanning electronic micrograph of the biologic scaffold in vitro. *A*: Plasma/thrombin mix. Fibrin polymerizes forming an intricate three-dimensional network (bar = 5 μm). *B*: Untreated human islet cell surface in culture medium (bar = 50 μm). *C*: Human islets embedded within the biologic scaffold. The polymerized fibrin forms an orthomorphic matrix around the islet surface (bar = 50 μm).

comparable glucose clearance at both time points (n = 5; AUC 19,542 ± 1,735 mg × min × dL^{-1} at 11 weeks and 20,735 ± 785 mg × min × dL^{-1} at 26 weeks) (Fig. 3*C*). Histopathology of explanted grafts showed well-preserved islet cytoarchitecture (Fig. 3*D*–*G*), strong insulin immunostaining, and abundant intragraft vascularization (e.g., SMA); all features were compatible with adequate engraftment and corroborated the in vivo functional data.

Comparable Function of Intrahepatic and Intraomental Islets Transplanted Into Biologic Scaffolds

We compared the performance of syngeneic islets implanted within the intraomental biologic scaffold to that of intrahepatic grafts. Aliquots of 1,300 IEQ (~8,200 IEQ/kg body wt [a "clinically relevant" mass]) from the same batch of islets were transplanted in parallel either within an intraomental biologic scaffold (n = 7; 160.3 ± 6.4 g body wt [8,122 ± 334 IEQ/kg]) (Fig. 4*A*) or in the

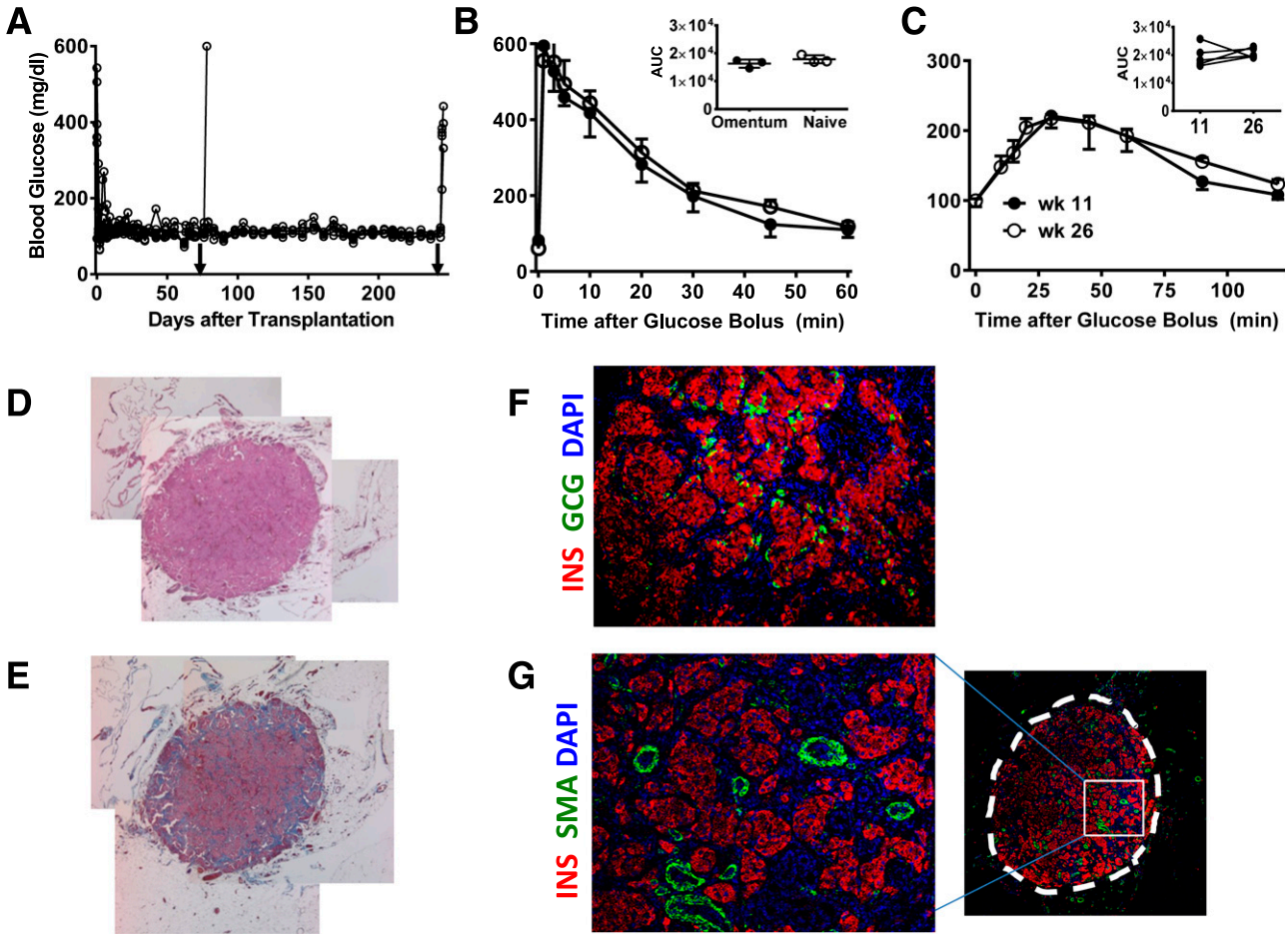

Figure 3—Intraomental islets transplanted into biologic scaffolds restore normoglycemia in diabetic rats. *A*: Nonfasting blood glucose levels in diabetic rats (n = 7; 173.4 ± 91 g body wt) transplanted with 3,000 IEQ (17,338 ± 881 IEQ/kg) onto the omentum showing prompt reversal of diabetes and hyperglycemia after removal of the omental graft (arrowhead) on POD 74 (n = 1) or 240 (n = 4). *B*: Glycemic profile during IVGTT performed in selected animals (n = 3) 2 months after transplant compared with that of naïve animals (n = 3). Values shown are mean ± SD. Inset shows area under the curve (AUC) (mg × min × dL^{-1}) for each group. *C*: Glycemic profile during OGTT performed in transplanted animals (n = 5) at 11 (●) and 26 (○) weeks after transplantation. Inset shows AUC (mg × min × dL^{-1}) during the glucose challenge. *D–G*: Representative histopathologic pattern of intraomental islet grafts. Sections were obtained from an intraomental islet graft explanted on POD 76. *D*: Hematoxylin-eosin staining. *E*: Masson trichrome staining. *F* and *G*: Immunofluorescence microscopy of a section stained with anti-insulin (INS) (red fluorescence), anti-GCG antibody (green fluorescence) (*F*), anti-SMA (green fluorescence) (*G*), and nuclear dye DAPI (blue fluorescence). The box indicates the area of the graft shown at higher magnification on the left panel. wk, week.

intrahepatic site (n = 5; 155.4 ± 7.3 g body wt [8,380 ± 396 IEQ/kg]) (Fig. 4*B*). All recipients in both groups achieved euglycemia within 1 week and maintained good metabolic control during the 82-day (~12 weeks) follow-up period. Omental graft removal resulted in a prompt return to hyperglycemia (n = 4) (Fig. 4*A*). At 5 (Fig. 4*C*) and 11 weeks posttransplant (Fig. 4*D*), OGTT showed comparable metabolic function in both transplant sites (AUC at 5 weeks, 18,393 ± 571 and 18,036 ± 598.5 mg × min × dL^{-1}, and AUC at 11 weeks, 21,987 ± 2,580 and 21,149 ± 1,456 mg × min × dL^{-1}, for intraomental biologic scaffold recipients or intrahepatic islet recipients, respectively) (Fig. 4*C* and *D*).

Lower Levels of Stress-Related Biomarkers in Recipients of Intraomental Islets Within a Biologic Scaffold

Selected biomarkers associated with islet distress and inflammation elicited by the transplantation procedure were evaluated. Blood samples were collected from JVC at different time points after transplantation. A spike in insulin and C-peptide levels, likely a result of insulin dumping from distressed islet cells (5,37,38), was observed 1 h posttransplant in both experimental groups. The insulin peak was significantly higher in the intrahepatic compared with the intraomental group (2.841 ± 0.338 vs. 1.405 ± 0.352 μg/mL, respectively; P = 0.018) (Fig. 5*A*), with comparable levels in both groups at subsequent time points (data not shown). No statistically significant differences were observed in C-peptide levels (2.565 ± 0.25 vs. 2.941 ± 0.303 μg/mL, respectively) (Fig. 5*B*).

Inflammatory biomarkers MCP-1/CCL2 (Fig. 5*C*) and IL-6 (Fig. 5*D*) showed comparable increases between experimental groups at 24 h, with undetectable values by 72 h posttransplant in both groups (not shown). Leptin levels were significantly higher at 24 h in the recipients of

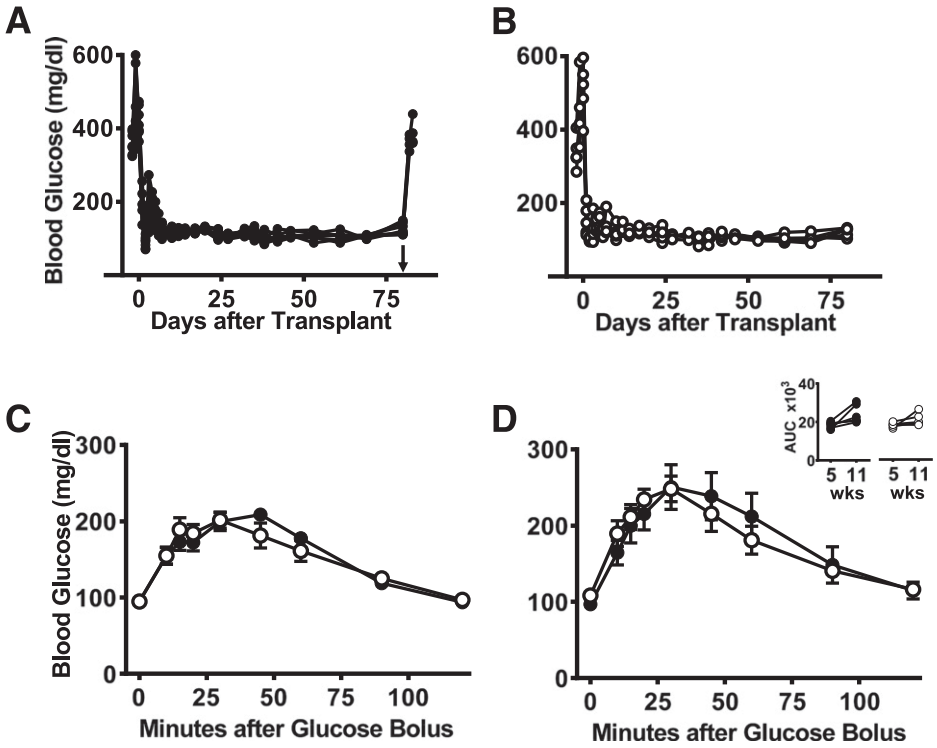

Figure 4—Comparable function of intrahepatic and intraomental islets transplanted into biologic scaffolds. Nonfasting blood glucose levels in diabetic rats receiving a clinically relevant syngeneic islet mass of 1,300 IEQ (~8,200 IEQ/kg body wt) within an intraomental biologic scaffold (*A*) (●, $n = 7$) or into the liver (via the portal vein) (*B*) (○, $n = 5$) with islets from the same batch isolation. The groups had an identical time course for reversal of diabetes, and removal of the intraomental biologic scaffold on day 80 posttransplant resulted in return to hyperglycemia (arrowhead in *A*). Glycemic profile during OGTT performed in all transplanted animals 5 (*C*) or 11 weeks (*D*) after transplantation. Inset shows AUC (mg × min × dL^{-1}) during the glucose challenge for each group. wks, weeks.

the intrahepatic compared with intraomental group (633 ± 31 vs. 483 ± 35 pg/mL, respectively; $P = 0.013$) (Fig. 5*E*). Acute-phase protein haptoglobin levels were comparable in both groups (Fig. 5*F*), while α2-macroglobulin levels were significantly higher in intrahepatic islet recipients versus the intraomental group at 24 h (280 ± 58 vs. 155 ± 26 pg/mL; one-tail *t* test: $P < 0.03$) (Fig. 5*G*).

Intraomental Biologic Scaffold Provides Adequate Engraftment of Low-Purity Islet Preparations

Clinical human islet preparations usually contain different degrees of impurities (e.g., exocrine tissue) that increase the final volume of transplanted tissue. We evaluated whether our intraomental biologic scaffold would be adequate for the implantation of clinically relevant, low-purity islet preparations. Implantation of 2,000 IEQ from either >95% pure ($n = 3$; 167.3 ± 1.5 g body wt [11,853 ± 109 IEQ/kg]) or 30% pure ($n = 3$; 170.3 ± 10.5 g body wt [11,771 ± 725 IEQ/kg]) syngeneic islet preparations led to rapid diabetes reversal (within 5 days) in all recipient rats (Fig. 6*A*). All animals maintained stable normoglycemia throughout the follow-up period and displayed comparable glucose clearance during OGTT (AUC: 17,776 ± 1,687 and 19,734 ± 1,997 mg × min × dL^{-1} for recipients of 90 and 30% pure preparations, respectively) (Fig. 6*B*). Surgical removal of the graft-bearing omentum was performed >100 days after transplantation. One of the recipients of 30% pure islets died after surgery, while all other animals in both groups showed prompt return to hyperglycemia, confirming the graft-dependent normoglycemia.

Intraomental Biologic Scaffold Provides Adequate Engraftment of Allogeneic Islets in Immunosuppressed Recipients

Suitability of the intraomental biologic scaffold to support islet engraftment under clinically relevant systemic immunosuppressive treatment (32–35) was evaluated in a fully MHC-mismatched allogeneic rat transplant combination. All four diabetic Lewis rat ($RT1^l$) recipients of 3,000 IEQ WF islets ($RT1^u$) achieved normoglycemia within 5 days and sustained graft function for up to 5 weeks posttransplantation under the transient systemic immunosuppression protocol used, when graft rejection coincided with return to a hyperglycemic state (Fig. 7).

Intraomental Islet Transplant in a Biologic Scaffold Engrafts in a Preclinical Model

We also tested the effect of the biologic scaffold in a clinically relevant preclinical model of allogeneic islet transplantation in a diabetic cynomolgus monkey. Before transplantation, the animal required ~4–5 IU/kg/day

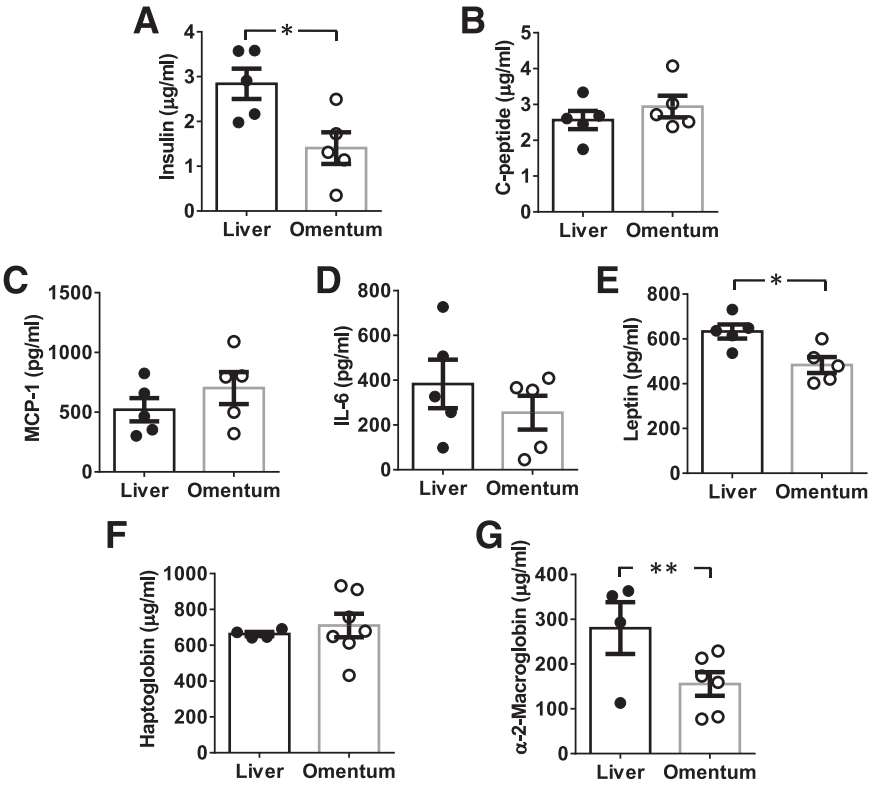

Figure 5—Biomarkers detected in the serum of rat recipients of intraomental biologic scaffold and intrahepatic syngeneic islets. Aliquots of 1,300 IEQ from the same syngeneic donor rat islet batch were transplanted in parallel either within the intraomental biologic scaffold (omentum [○]) or the intrahepatic site (liver [●]). Blood samples were collected from indwelling JVC for detection of biomarker levels in circulation. Data presented are mean ± SEM (n = 4–7 per time point). *A* and *B*: Metabolic markers assessed at 1 h posttransplant. *A*: Insulin in μg/mL (*P = 0.018). *B*: C-peptide in μg/mL. Inflammation markers assessed 24 h posttransplant: MCP-1/CCL2 in pg/mL (*C*), IL-6 in pg/mL (*D*), leptin in pg/mL (*P = 0.013) (*E*), haptoglobin in μg/mL (*F*), and α2-macroglobulin in μg/mL (**P < 0.03) (*G*).

exogenous insulin with plasma C-peptide <0.05 ng/mL (Fig. 8). An islet mass of ~48,700 IEQ (~150 μL total islet graft volume) equivalent to 9,347 IEQ/kg was implanted. The transplant procedure and postoperative clinical outcome were uneventful, with standard recovery from surgery. After the first few weeks posttransplant, improvement of FBG and PBG was observed, requiring progressive reduction of exogenous insulin (Fig. 8*A*). Positive fasting C-peptide levels (Fig. 8*B*) were observed immediately posttransplant and throughout follow-up. The animal subsequently expired on postoperative day (POD) 49 owing to technical complications unrelated to the engraftment site. Histopathologic assessment of the explanted graft demonstrated well-preserved islet morphology (Fig. 8*C*) with immunoreactivity for the endocrine markers insulin and glucagon (Fig. 8*D*), some degree of peri-insular lymphocyte infiltrate (CD3) (Fig. 8*E*), and abundant intra- and extrainsular vascular structures (SMA [Fig. 8*F*] and vWF [Fig. 8*G*]).

DISCUSSION

Our study was aimed at developing a clinically applicable protocol for extrahepatic transplantation of pancreatic islets. Over the past 20 years, the omentum has been studied as a possible islet implantation site in different animal models, after the initial description by Yasunami et al. (39) using rat isografts and later reports in large animals (40–42). Owing to portal venous drainage, the omentum may attain more physiologic metabolic responses compared with intrahepatic and other islet transplantation sites that were associated with hyperinsulinemia, insulin resistance, and impairment of insulin action in animal models (20,21,23). Human islet cell implants survived better in the omentum than intrahepatically in immunodeficient rats, and their engraftment correlated positively with number and purity of implanted cells (43). Perinatal porcine islet cells displayed comparable growth of the β-cell volume over time in the omentum and kidney subcapsular space, the former leading to higher insulin reserves and an increased pool of proliferating cells (44). These data reinforce the feasibility of the omentum as a potentially favorable site for the implantation of insulin-producing cell products in clinical protocols.

From the clinical translational perspective, the omentum can be accessed using minimally invasive surgical techniques (e.g., minilaparotomy or laparoscopy), and it may allow implementation of bioengineering approaches

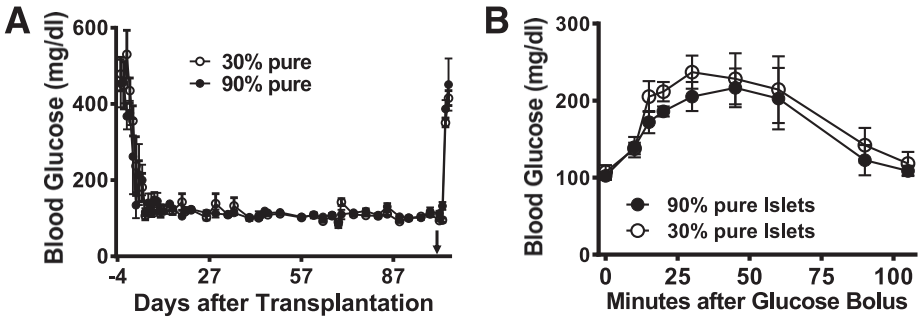

Figure 6—Intraomental transplantation of islets with high and low purity into diabetic rats. *A*: Nonfasting blood glucose levels in diabetic rats transplanted with clinically relevant mass of 2,000 IEQ syngeneic islets with >95% purity (n = 3) (167.3 ± 1.5 g body wt [11,853 ± 109 IEQ/kg]) or with 30% purity (n = 3) (170.3 ± 10.5 g body wt [11,771 ± 725 IEQ/kg]) onto the omentum. Removal of the omental graft >100 days after transplantation (arrowhead) resulted in return to hyperglycemia. *B*: Glycemic profile during oral glucose tolerance test performed in animals transplanted with high-purity and low-purity islet preparations 70 days after transplantation.

to enhance islet engraftment, survival, and development of strategies for the reduction and eventual elimination of chronic systemic immunosuppression of the recipients (14,22,45). We evaluated the potency of islets implanted onto the omentum using an autologous resorbable biologic scaffold to promote islet adherence onto its surface using only clinical grade reagents (e.g., rhT). The clinical safety profile of rhT has been established to promote hemostasis during surgical procedures (46). We reasoned that applying islets suspended in autologous plasma on the surface of the omentum would accommodate relatively large islet volumes while minimizing pelleting. A similar approach based on three-dimensional islet-plasma constructs prepared ex vivo and then rolled up within the greater omentum was described in pancreatectomized dogs (47).

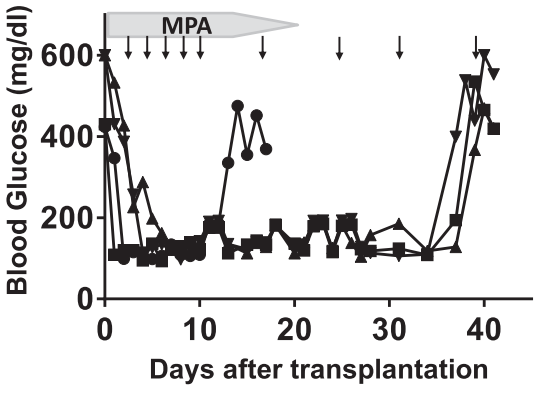

Figure 7—The intraomental biologic scaffold supports the engraftment of allogeneic islets under systemic immunosuppression in diabetic rats. A fully MHC-mismatched allogeneic rat transplant combination in which diabetic female Lewis rat (RT1^l) (n = 4) received 3,000 IEQ WF rat islets (RT1^u) in the intraomental biologic scaffold under a protocol of clinically relevant immunosuppressive agents consisting of lymphodepletion induction with anti-lymphocyte serum (0.5 mL i.p. on day −3) and maintenance with mycophenolic acid (MPA) (20 mg/kg/day for days 0–14, then tapered by one-quarter of the dose every 2 days until day 20) and CTLA4Ig (10 mg/kg i.p. on days 0, 2, 4, 6, 8, and 10 and weekly thereafter; abatacept) (arrows). Nonfasting glycemic values for each animal during the follow-up are presented. Graft rejection was defined as return to hyperglycemic state. Each symbol represents an individual animal.

Our in vitro results showed that addition of rhT to human islets resuspended in human plasma generates a complex, orthomorphic fibrin matrix embedding the islets. Our in vivo studies demonstrate that islets transplanted in the in situ–generated biologic scaffold onto the omentum of diabetic animals engraft and function long-term. Normalization of nonfasting glycemic values and responses during metabolic challenges were reproducibly achieved in recipients of syngeneic islets in an intraomental biologic scaffold. Histopathology showed preserved islet cytoarchitecture in the presence of rich intrainsular vascular structures and lack of fibrosis in both rodent and NHP models. Moreover, when adequate islet numbers were implanted in the rat model (i.e., >1,300 IEQ; ~8,200/kg body wt), there was comparable potency between intraomental and intrahepatic transplants. However, a higher proportion of intrahepatic islet recipients achieved metabolic control when a marginal (though not clinically relevant) syngeneic rat islet mass of 450 IEQ, representing ~2,700/kg body wt, was implanted (data not shown). It is noteworthy that 5,000 IEQ/kg body wt is currently the minimum requirement for clinical intrahepatic islet transplantation, and insulin independence is generally attained when >12,000 IEQ/kg are implanted (1).

Serum levels of insulin and C-peptide, surrogate biomarkers of acute β-cell distress and death associated with the implantation procedure (5,37,38), were increased 1 h postimplant, with higher levels in recipients of intrahepatic versus intraomental islets. Perhaps the lower intraomental levels are due, at least in part, to the lack of shear forces and IBMIR in this site (4,6). While the kinetics for appearance of the inflammatory markers IL-6, MCP-1/CCL2, and haptoglobin were comparable, α2-macroglobulin levels were higher 24 h after intrahepatic versus intraomental transplantation. Notably, the pleomorphic plasma protein α2-macroglobulin interfaces

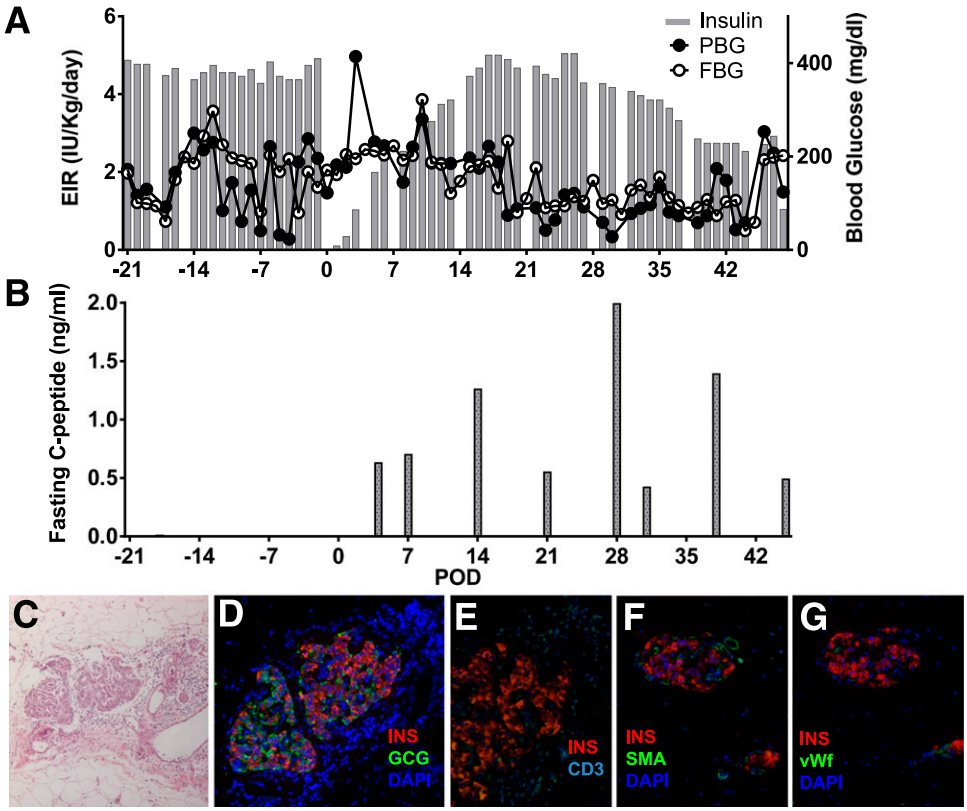

Figure 8—Intraomental allogeneic islet transplantation in a diabetic nonhuman primate. A diabetic cynomolgus monkey received 9,347 IEQ/kg allogeneic islets in the omentum under the cover of clinically relevant immunosuppression therapy. *A*: Exogenous insulin requirement (EIR) (IU/kg/day), FBG (mg/dL), and PBG. *B*: Fasting C-peptide (ng/mL) levels measured in the animal over the follow-up period. *C*–*G*: Histopathologic pattern of intraomental islet graft on day 49 posttransplant. *C*: Hematoxylin-eosin staining. *D*: Immunofluorescence microscopy for the evaluation of immunoreactivity for insulin (INS) (red), GCG (green), and nuclear dye (DAPI) (blue). *E*: Immunofluorescence for insulin (red) and $CD3^+$ T cells (CD3) (cyan). *F* and *G*: Intrainsular neovasculogenesis. *F*: Immunofluorescence for insulin (red), vascular structure (SMA) (green), and DAPI (blue). *G*: Immunofluorescence microscopy for insulin (red), endothelial cells (vWF) (green), and DAPI (blue).

with the coagulation system and is an acute-phase protein (48). This result may be due to hepatic tissue responses after islet embolization in the portal system (i.e., Kupffer cell activation and in the context of thrombi). Levels of leptin, a mediator of innate immunity through multiple proinflammatory effects (49), increased in both groups but were higher in the intrahepatic compared with the intraomental islet recipients, reaching statistical significance at the 24-h time point. Collectively, these data suggest a lower degree of inflammation generated after intraomental islet implantation in the biologic scaffold compared with the liver.

Antithrombin agents have been proposed to reduce IBMIR and promote intrahepatic islet engraftment (50). Our data indicate that thrombin per se is not detrimental to islet engraftment when used in an extravascular (extrahepatic) site to induce a resorbable matrix in vivo. This is likely due to the absence of the plethora of proinflammatory events associated with intravascular thrombosis in the hepatic sinusoids, including transplant microenvironment activation (platelets, leukocytes, and endothelial cells), that lead to islet hypoxia and loss of functional islet mass.

Human islet preparations generally include low-purity fractions of the final cellular product to achieve adequate endocrine cell mass for transplantation. However, the final volume of clinical human islet preparations implanted is generally kept <10 mL to reduce the risk of portal vein hypertension after embolization in the liver sinusoids. The net effect of the inclusion of exocrine fractions in the islet transplant preparation remains to be determined (51). Exocrine tissue may be detrimental to islet graft outcome because of competition for nutrients and oxygen in the transplant site, contribution to microenvironment activation, and increased antigenic mass transplanted. Conversely, exocrine tissue may comprise critical cellular precursors that promote engraftment, tissue remodeling, and endocrine cell plasticity, leading to long-term function after transplantation (52,53). In light of the promising long-term results of autologous intrahepatic human islet grafts (not or minimally purified) (54), development of extrahepatic implantation sites that accommodate impure islet preparations represents a desirable goal for clinical islet transplantation (14,15,55). In this study, transplantation of islet preparations with low purity (30% endocrine)

resulted in stable metabolic control that was comparable with that of pure preparations (>95% endocrine) transplanted into the biologic intraomental scaffold.

Our preclinical studies of islet transplantation support the feasibility of intraomental transplantation of islets using the described in situ–generated biologic scaffold. Using both rat and NHP models, we demonstrated that allogeneic islets implanted in the intraomental biologic scaffold under clinically relevant immunosuppression (32) can engraft and improve glucose control and that this procedure may be feasible and effective in human subjects. The implantation procedure that we have optimized allows for distribution of the grafted tissue on the large omental surface and the creation of a thin adherent biologic scaffold in situ with minimal manipulation, avoiding islet pelleting (even in the case of low-purity cell products). Folding of an omental flap on the scaffold creates a double outer omental layer containing the graft, increasing surface contact (for nutrient diffusion and subsequent neovascularization), and protecting the islets from shear forces (peristalsis and diaphragm excursions) in the peritoneal cavity. The use of only two components (namely, the patient's own plasma and rhT) to generate a resorbable biologic scaffold and the simplicity of the implantation technique make our approach easy to implement and clinically translatable. Furthermore, it may represent an initial step toward engineering the transplant site to enhance β-cell replacement therapies for insulin-requiring diabetes (14,22,45). A phase I/II pilot clinical trial is currently ongoing at our center to evaluate the safety and efficacy of transplanting single-donor allogeneic islets in biologic intraomental scaffolds under conventional immunosuppression in people with brittle T1D.

Acknowledgments. The authors thank Paul Latta (Converge Biotech); the faculty and staff of the DRI's Cell Transplant Center, particularly Dr. Rodolfo Alejandro and Dr. Luca Inverardi; Christian La Sala (DRI Preclinical Cell Processing and Translational Models Program); Dr. Joel Szust, Alejandro Tamayo-Garcia, Yelena Gadea, and Elsie Zahr-Akrawi (DRI Translational Core); Kevin Johnson (DRI Histology Lab); Dr. Patricia L. Blackwelder (UM Center for Advanced Microscopy); Dr. Marcia Boulina (DRI Imaging Core); Dr. Elina Linetsky (DRI cGMP Human Cell Processing Core); Waldo Diaz, James Geary, and Reiner Rodriguez-Lopez for excellent NHP care; and Alexander Rabassa, Ena Poumian-Ruiz, and Melissa Willman for assistance with NHP islet isolation and preliminary in vitro testing. The authors give special thanks to the UM Institutional Animal Care and Use Committee, UM Office of Environmental Health and Safety, and Division of Veterinary Resources for valuable support provided.

Funding. This study was partially supported by the Diabetes Research Institute Foundation (www.diabetesresearch.org), by the Leona M. and Harry B. Helmsley Charitable Trust, and by JDRF International (17-2012-361). The project was part of A.P.'s Master of Science in Clinical and Translational Investigation training, a program supported by the UM Clinical and Translational Science Institute, from the National Center for Advancing Translational Sciences and the National Institute on Minority Health and Health Disparities (1UL1TR000460).

The contents of this article are solely the responsibility of the authors and do not necessarily represent the official views of the funding agencies. The opinions expressed in this article are the authors' own and do not reflect the view of the National Institutes of Health, the Department of Health and Human Services, or the U.S. government.

Duality of Interest. UM and R.D.M., N.S.K., C.R., and A.P. hold, but do not receive royalties for, intellectual property used in this study and are also equity owners in Converge Biotech. No other potential conflicts of interest relevant to this article were reported.

Author Contributions. D.M.B., C.R., and A.P. developed the concept. D.M.B., R.D.M., C.R., and A.P. conceived and designed the studies, performed experiments, optimized protocols, analyzed data, and wrote the manuscript. C.F., N.M.K., and N.S.K. performed experiments, analyzed data, provided intellectual input, and reviewed the manuscript. U.U. and J.G. performed experiments, analyzed data, and reviewed the manuscript. A.J.M. and D.M.A. provided intellectual feedback and reviewed the manuscript. C.R. and A.P. are the guarantors of this work and, as such, had full access to all the data in the study and take responsibility for the integrity of the data and the accuracy of the data analysis.

Prior Presentation. Parts of this study were presented in abstract form at the 12th Congress of the Cell Transplant Society, Milan, Italy, 7–11 July 2013, and at the 75th Scientific Sessions of the American Diabetes Association, Boston, MA, 5–9 June 2015.

References

1. Piemonti L, Pileggi A. 25 years of the Ricordi Automated Method for islet isolation. CellR4 2013;1:8–22
2. Pileggi A, Ricordi C, Kenyon NS, et al. Twenty years of clinical islet transplantation at the Diabetes Research Institute–University of Miami. Clin Transpl 2004;177–204
3. Alejandro R, Cutfield RG, Shienvold FL, et al. Natural history of intrahepatic canine islet cell autografts. J Clin Invest 1986;78:1339–1348
4. Bennet W, Groth CG, Larsson R, Nilsson B, Korsgren O. Isolated human islets trigger an instant blood mediated inflammatory reaction: implications for intraportal islet transplantation as a treatment for patients with type 1 diabetes. Ups J Med Sci 2000;105:125–133
5. Moberg L, Johansson H, Lukinius A, et al. Production of tissue factor by pancreatic islet cells as a trigger of detrimental thrombotic reactions in clinical islet transplantation. Lancet 2002;360:2039–2045
6. Johansson H, Lukinius A, Moberg L, et al. Tissue factor produced by the endocrine cells of the islets of Langerhans is associated with a negative outcome of clinical islet transplantation. Diabetes 2005;54:1755–1762
7. Berman DM, Cabrera O, Kenyon NM, et al. Interference with tissue factor prolongs intrahepatic islet allograft survival in a nonhuman primate marginal mass model. Transplantation 2007;84:308–315
8. Markmann JF, Rosen M, Siegelman ES, et al. Magnetic resonance-defined periportal steatosis following intraportal islet transplantation: a functional footprint of islet graft survival? Diabetes 2003;52:1591–1594
9. Bhargava R, Senior PA, Ackerman TE, et al. Prevalence of hepatic steatosis after islet transplantation and its relation to graft function. Diabetes 2004;53:1311–1317
10. Eckhard M, Lommel D, Hackstein N, et al. Disseminated periportal fatty degeneration after allogeneic intraportal islet transplantation in a patient with type 1 diabetes mellitus: a case report. Transplant Proc 2004;36:1111–1116
11. Maffi P, Angeli E, Bertuzzi F, et al. Minimal focal steatosis of liver after islet transplantation in humans: a long-term study. Cell Transplant 2005;14:727–733
12. Leitão CB, Peixoto EM, Westphalen AC, et al. Liver fat accumulation after islet transplantation and graft survival. Cell Transplant 2014;23:1221–1227
13. Jackson S, Mager DR, Bhargava R, et al. Long-term follow-up of hepatic ultrasound findings in subjects with magnetic resonance imaging defined hepatic steatosis following clinical islet transplantation: a case-control study. Islets 2013;5:16–21
14. Fotino N, Fotino C, Pileggi A. Re-engineering islet cell transplantation. Pharmacol Res 2015;98:76–85
15. Pileggi A, Ricordi C. A new home for pancreatic islet transplants: the bone marrow. Diabetes 2013;62:3333–3335
16. Philosophe B, Farney AC, Schweitzer EJ, et al. Superiority of portal venous drainage over systemic venous drainage in pancreas transplantation: a retrospective study. Ann Surg 2001;234:689–696

17. Platell C, Cooper D, Papadimitriou JM, Hall JC. The omentum. World J Gastroenterol 2000;6:169–176
18. Chaffanjon PC, Kenyon NM, Ricordi C, Kenyon NS. Omental anatomy of non-human primates. Surg Radiol Anat 2005;27:287–291
19. Ackermann PC, De Wet PD, Loots GP. Microcirculation of the rat omentum studied by means of corrosion casts. Acta Anat (Basel) 1991;140:146–149
20. Guan J, Zucker PF, Atkison P, Behme MT, Dupre J, Stiller CR. Liver-omental pouch and intrahepatic islet transplants produce portal insulin delivery and prevent hyperinsulinemia in rats. Transplant Proc 1995;27:3236
21. Guan J, Behme MT, Zucker P, et al. Glucose turnover and insulin sensitivity in rats with pancreatic islet transplants. Diabetes 1998;47:1020–1026
22. Berman DM, O'Neil JJ, Coffey LC, et al. Long-term survival of nonhuman primate islets implanted in an omental pouch on a biodegradable scaffold. Am J Transplant 2009;9:91–104
23. Kim HI, Yu JE, Park CG, Kim SJ. Comparison of four pancreatic islet implantation sites. J Korean Med Sci 2010;25:203–210
24. Perez VL, Caicedo A, Berman DM, et al. The anterior chamber of the eye as a clinical transplantation site for the treatment of diabetes: a study in a baboon model of diabetes. Diabetologia 2011;54:1121–1126
25. Pileggi A, Molano RD, Ricordi C, et al. Reversal of diabetes by pancreatic islet transplantation into a subcutaneous, neovascularized device. Transplantation 2006;81:1318–1324
26. Ichii H, Pileggi A, Molano RD, et al. Rescue purification maximizes the use of human islet preparations for transplantation. Am J Transplant 2005;5:21–30
27. Hogan AR, Doni M, Molano RD, et al. Beneficial effects of ischemic preconditioning on pancreas cold preservation. Cell Transplant 2012;21:1349–1360
28. Ricordi C, Lacy PE, Finke EH, Olack BJ, Scharp DW. Automated method for isolation of human pancreatic islets. Diabetes 1988;37:413–420
29. Ricordi C. Islet transplantation: a brave new world. Diabetes 2003;52:1595–1603
30. Purified human pancreatic islets (PHPI) master production batch record – a standard operating procedure of the NIH Clinical Islet Transplantation Consortium. CellR4 2014;2:e891
31. Pileggi A, Ribeiro MM, Hogan AR, et al. Impact of pancreatic cold preservation on rat islet recovery and function. Transplantation 2009;87:1442–1450
32. Posselt AM, Szot GL, Frassetto LA, et al. Islet transplantation in type 1 diabetic patients using calcineurin inhibitor-free immunosuppressive protocols based on T-cell adhesion or costimulation blockade. Transplantation 2010;90:1595–1601
33. Vergani A, D'Addio F, Jurewicz M, et al. A novel clinically relevant strategy to abrogate autoimmunity and regulate alloimmunity in NOD mice. Diabetes 2010;59:2253–2264
34. Badell IR, Russell MC, Cardona K, et al. CTLA4Ig prevents alloantibody formation following nonhuman primate islet transplantation using the CD40-specific antibody 3A8. Am J Transplant 2012;12:1918–1923
35. Safley SA, Cui H, Cauffiel SM, Xu BY, Wright JR Jr, Weber CJ. Encapsulated piscine (tilapia) islets for diabetes therapy: studies in diabetic NOD and NOD-SCID mice. Xenotransplantation 2014;21:127–139
36. Brady AC, Ricordi C, Molano RD, et al. Local immumosuppression modulates islet allograft rejection into a biohybrid device. Am J Transplant 2010;10:76–77
37. Faradji RN, Monroy K, Cure P, et al. C-peptide and glucose values in the peritransplant period after intraportal islet infusions in type 1 diabetes. Transplant Proc 2005;37:3433–3434
38. Berney T, Mamin A, James Shapiro AM, et al. Detection of insulin mRNA in the peripheral blood after human islet transplantion predicts deterioration of metabolic control. Am J Transplant 2006;6:1704–1711
39. Yasunami Y, Lacy PE, Finke EH. A new site for islet transplantation–a peritoneal-omental pouch. Transplantation 1983;36:181–182
40. Simeonovic CJ, Dhall DP, Wilson JD, Lafferty KJ. A comparative study of transplant sites for endocrine tissue transplantation in the pig. Aust J Exp Biol Med Sci 1986;64:37–41
41. Ao Z, Matayoshi K, Yakimets WJ, Katyal D, Rajotte RV, Warnock GL. Development of an omental pouch site for islet transplantation. Transplant Proc 1992;24:2789
42. Ao Z, Matayoshi K, Lakey JR, Rajotte RV, Warnock GL. Survival and function of purified islets in the omental pouch site of outbred dogs. Transplantation 1993;56:524–529
43. Jacobs-Tulleneers-Thevissen D, Bartholomeus K, Suenens K, et al. Human islet cell implants in a nude rat model of diabetes survive better in omentum than in liver with a positive influence of beta cell number and purity. Diabetologia 2010;53:1690–1699
44. Bartholomeus K, Jacobs-Tulleneers-Thevissen D, Shouyue S, et al. Omentum is better site than kidney capsule for growth, differentiation, and vascularization of immature porcine β-cell implants in immunodeficient rats. Transplantation 2013;96:1026–1033
45. Pedraza E, Brady AC, Fraker CA, et al. Macroporous three-dimensional PDMS scaffolds for extrahepatic islet transplantation. Cell Transplant 2013;22:1123–1135
46. Ham SW, Lew WK, Weaver FA. Thrombin use in surgery: an evidence-based review of its clinical use. J Blood Med 2010;1:135–142
47. Hefty TR, Kuhr CS, Chong KT, et al. Omental roll-up: a technique for islet engraftment in a large animal model. J Surg Res 2010;161:134–138
48. Cray C, Zaias J, Altman NH. Acute phase response in animals: a review. Comp Med 2009;59:517–526
49. Procaccini C, Pucino V, De Rosa V, Marone G, Matarese G. Neuro-endocrine networks controlling immune system in health and disease. Front Immunol 2014;5:143
50. Ozmen L, Ekdahl KN, Elgue G, Larsson R, Korsgren O, Nilsson B. Inhibition of thrombin abrogates the instant blood-mediated inflammatory reaction triggered by isolated human islets: possible application of the thrombin inhibitor melagatran in clinical islet transplantation. Diabetes 2002;51:1779–1784
51. Ichii H, Miki A, Yamamoto T, et al. Characterization of pancreatic ductal cells in human islet preparations. Lab Invest 2008;88:1167–1177
52. Ricordi C, Alejandro R, Rilo HH, et al. Long-term in vivo function of human mantled islets obtained by incomplete pancreatic dissociation and purification. Transplant Proc 1995;27:3382
53. Street CN, Lakey JR, Shapiro AM, et al. Islet graft assessment in the Edmonton Protocol: implications for predicting long-term clinical outcome. Diabetes 2004;53:3107–3114
54. Chinnakotla S, Bellin MD, Schwarzenberg SJ, et al. Total pancreatectomy and islet autotransplantation in children for chronic pancreatitis: indication, surgical techniques, postoperative management, and long-term outcomes. Ann Surg 2014;260:56–64
55. Kakabadze Z, Gupta S, Pileggi A, et al. Correction of diabetes mellitus by transplanting minimal mass of syngeneic islets into vascularized small intestinal segment. Am J Transplant 2013;13:2550–2557